# SUPPLEMENTARY INFORMATION

## Index:

# Data acquisition

The spectra used to further the assignments are listed below and were all collected at the high K+/high pH sample condition: 50mM K+/pH=7.5.

1) NcaCX and NcoCX truncated 3Ds (both 25ms and 100ms DARR-mix)
2) NCACX 3D
3) NCOCX 3D
4) 15ms C-C homonuclear (DARR)
5) 250 ms C-C homonuclear (DARR)

All spectra were acquired using a 4mm, triple channel, HXY probe spinning at 14Khz on the 750MHz Bruker Console at the NYSBC. Details of data acquisition for the triple resonance experiments are listed in Tables 1 and 2.

Carbon 50khz =-1db

Nitrogen 50Khz = -3.3db

Proton 100Khz = 0db

| Parameter | | NcaCX | NcoCX |
|---|---|---|---|
| H -> N CP | FS of H | -3db at 100% | -3db at 100% |
| | FS of N | -3.5db | -3.5db |
| | Ramp (on H) | Tangential | Tangential |
| | Ct | 1ms | 1ms |
| | Ct for prolines | 5ms | 5ms |
| | | | |
| N -> C | FS of N | -1.2db | 4.0db |
| | FS of C | 8.40db at 100% | -4.4db at 100% |
| | Ramp (on C) | Tangential | Tangential |
| | Ct (ms) | 8ms | 8ms |
| | | | |
| C -> C mixing | Mixing time (ms) | 25ms | 25ms |
| | proton power | 17db | 17db |
| | | | |
| Points | C | 3840 | 3840 |
| | N | 256 | 256 |
| | | | |
| Acq. Time (ms) | C | 20ms | 20ms |
| Approx. | N | 10ms | 10ms |
| | | | |
| Sweepwidth | C | 500ppm | 500ppm |

| | | | |
|---|---|---|---|
| | N | 200ppm | 200ppm |
| | | | |
| Carrier Freq | C | 40ppm | 180ppm |
| | N | 100ppm | 100ppm |

Table 1: Parameters for the N-C 2Ds

| Parameter | | NCACX | NCOCX |
|---|---|---|---|
| H -> N CP | FS of H | -3db at 100% | -3db at 100% |
| | FS of N | -3.5db | -3.5db |
| | Ramp (on H) | Tangential | Tangential |
| | Ct (ms) | 1.0 | 1.0 |
| | | | |
| N -> C | FS of N | -1.2db | 4.0db |
| | FS of C | 8.40db at 100% | -4.4db at 100% |
| | Ramp (on C) | Tangential | Tangential |
| | Ct (ms) | 8ms | 8ms |
| | | | |
| C -> C mixing | Mixing time (ms) | 25ms | 25ms |
| | proton power | 17db | 17db |
| | | | |
| Points | C (direct) | 3840 | 3840 |
| | C (indirect) | 48 | 60 |
| | N | 32 | 56 |
| | | | |
| Acq. Time (ms) | C (direct) | 20ms | 20ms |
| Approx. | C (indirect) | 4.2ms | 8 ms |
| | N | 3ms | 5 ms |
| | | | |
| Sweepwidth | C (direct) | 500ppm | 500ppm |
| | C (indirect) | 40ppm | 20ppm |
| | N | 70ppm | 70ppm |
| | | | |
| Carrier Freq | C | 50ppm | 175ppm |
| | N | 110ppm | 110ppm |

Table 2: Parameters for the N-C-C 3Ds.

**Data Processing:**

The 3D data were acquired in blocks and then added together before processing. The 2D data were acquired at a stretch. All data were processed using NMRPipe. The carbon dimensions were referenced externally using Adamantane, whose downfield shift was set to 40.48ppm

relative to DSS. The nitrogen dimensions were referenced externally to Glycine, whose amine nitrogen was set to 32.06ppm relative to DSS. The spectra were referenced by adjusting the carrier frequency in the process script. Spectra were slightly shifted to align in Sparky as needed.

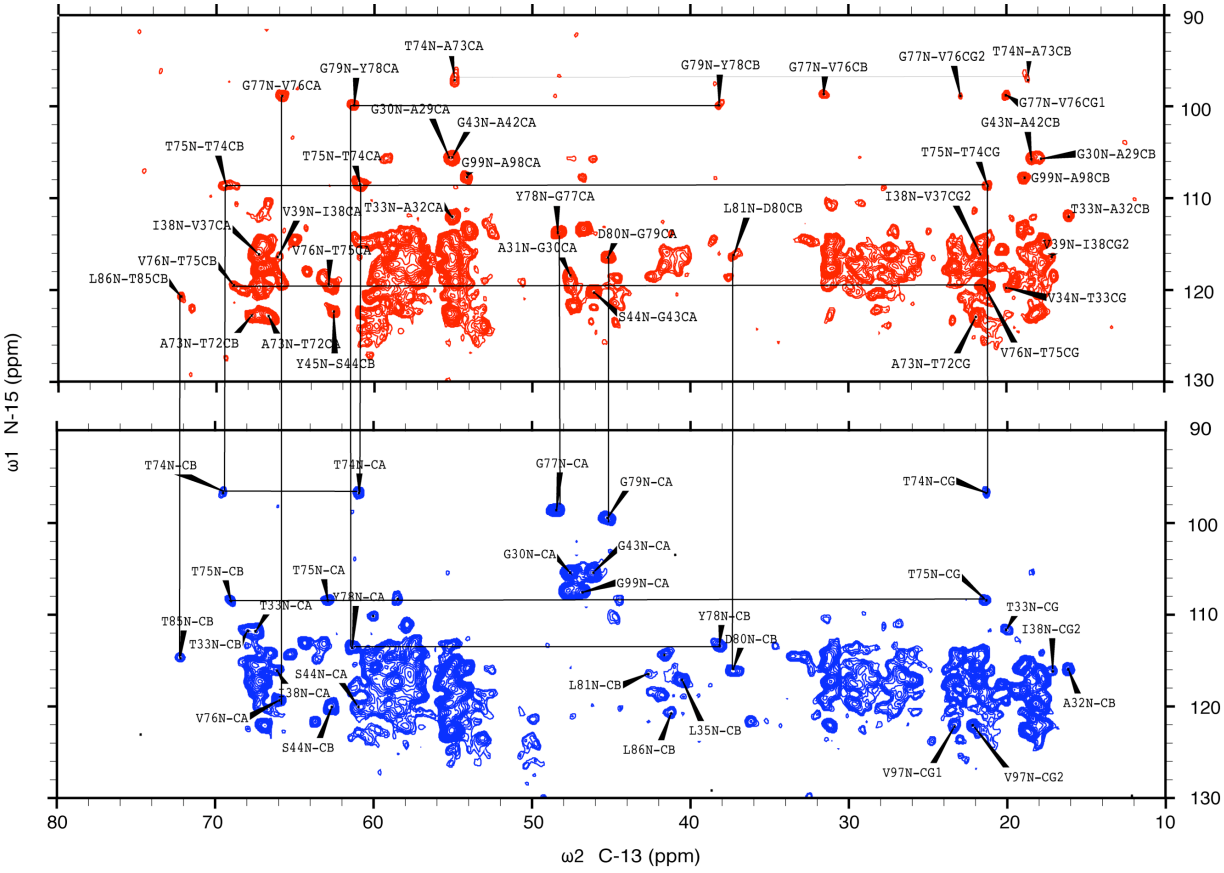


Fig. S.1. The backbone walk through the selectivity filter residues T74-D80 via NcaCX (blue) and NcoCX (red) heteronuclear correlation experiments. These data were collected on KcsA reconstituted into DOPE/DOPS bilayer at a [K+] of 50 mM and pH = 7.5.

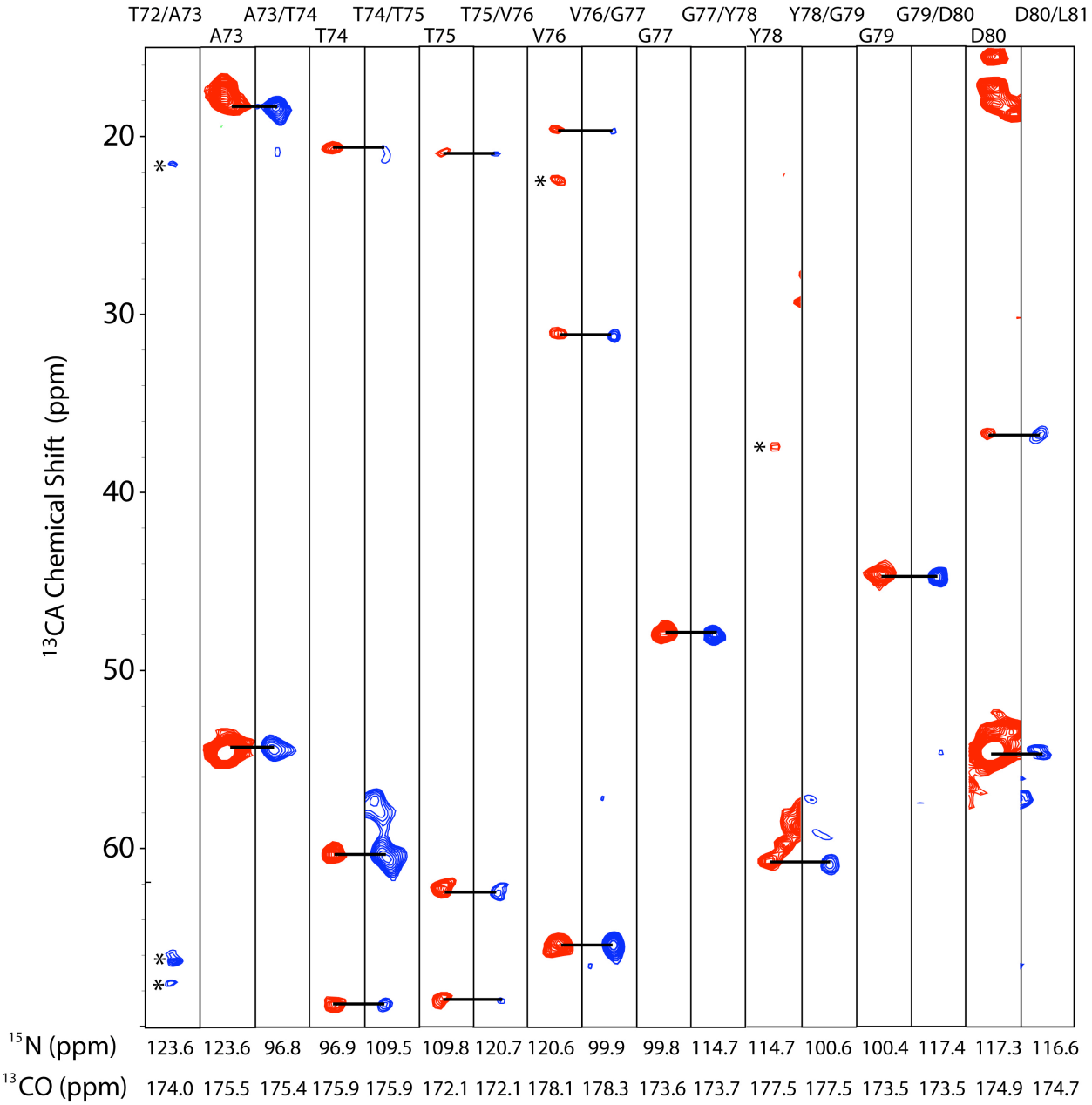


Fig. S.2. The backbone walk through the selectivity residues T74-D80 via NCOCX (blue) and NCACX (red) heteronuclear 3D correlation experiments. These data were collected on KcsA reconstituted into DOPE/DOPS bilayer at a [K+] of 50 mM and pH = 7.5.

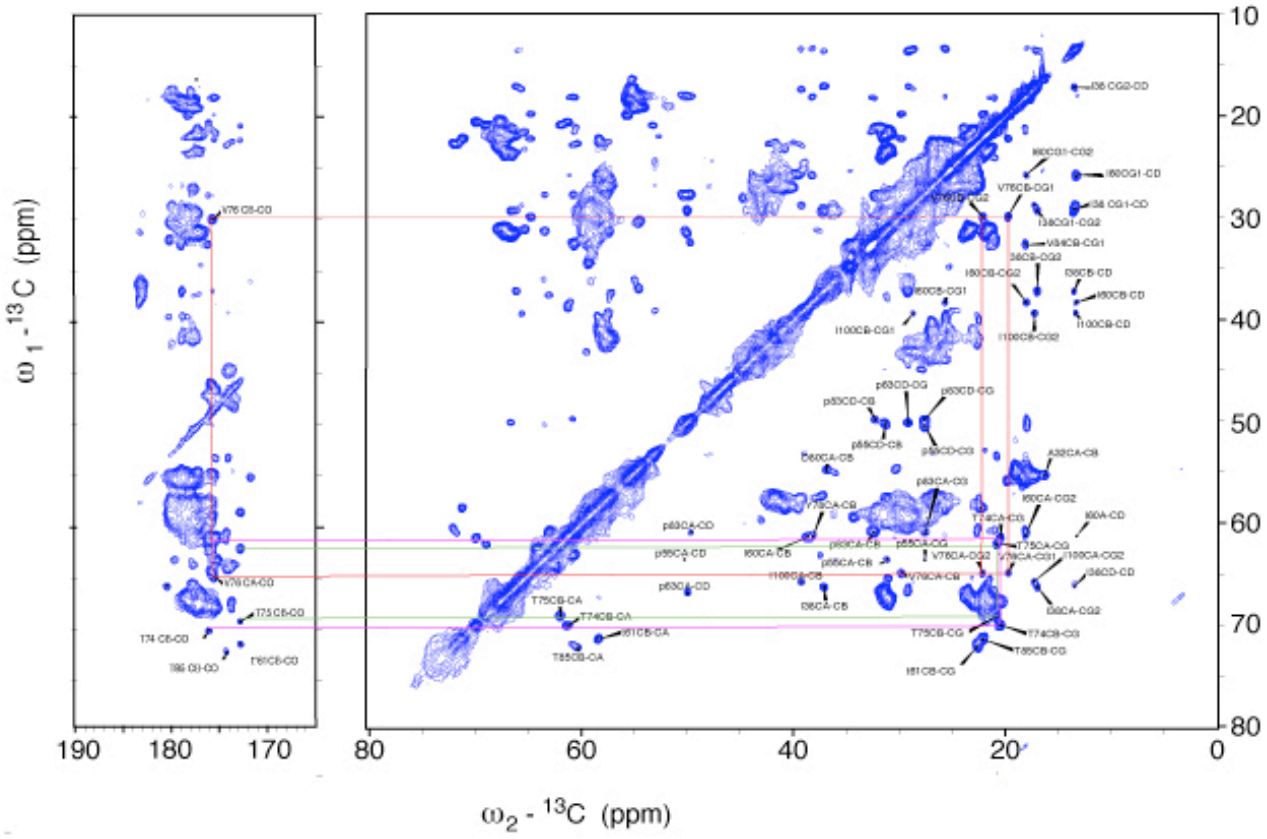


Fig. S.3. Many residues are resolved on a CC homonuclear 2D at low $K^+$. This figure shows the CC2D (15ms DARR) spectra of KcsA reconstituted into DOPE/DOPS bilayers at [$K^+$] = 0mM and pH= 7.5.

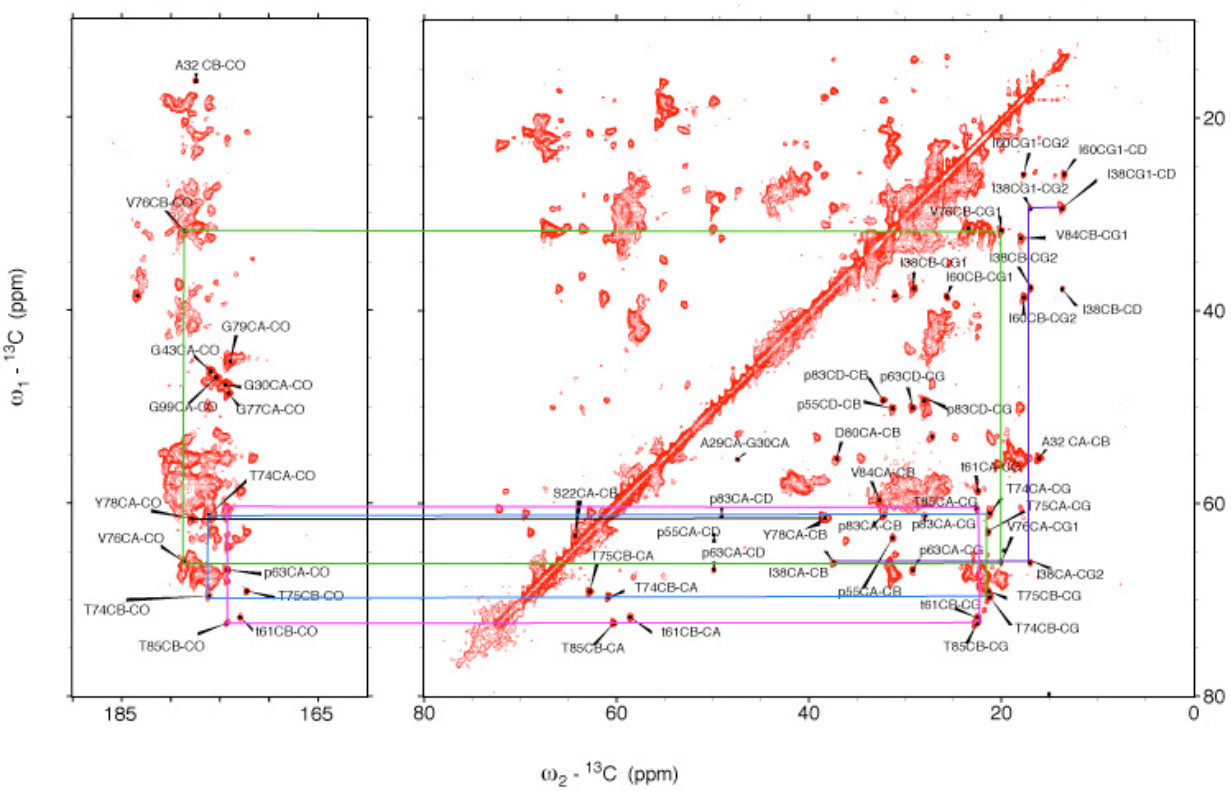


Fig. S4. Many residues are resolved on a CC homonuclear 2D at high $K^+$. This figure shows the CC2D (15ms DARR) spectra of KcsA reconstituted into DOPE/DOPS bilayers at [$K^+$] = 0mM and pH= 7.5.

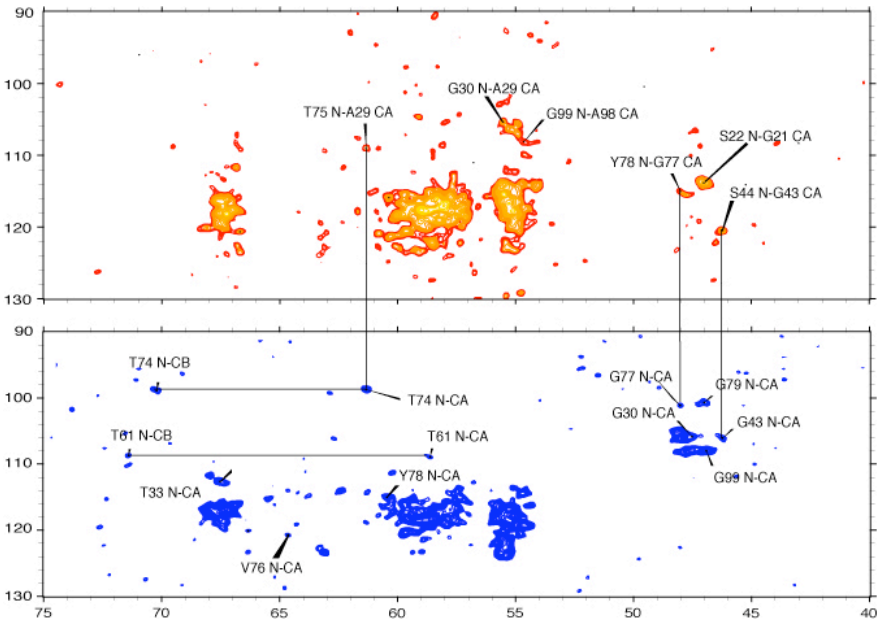


Fig. S5. Partial assignments of the selectivity filter residues T74-G79 in the low $K^+$ state via NcaCX (blue) and NcoCX (red) heteronuclear correlation experiments. These data were collected on KcsA reconstituted into DOPE/DOPS bilayer at a [K+] of 50 mM and pH = 7.5.

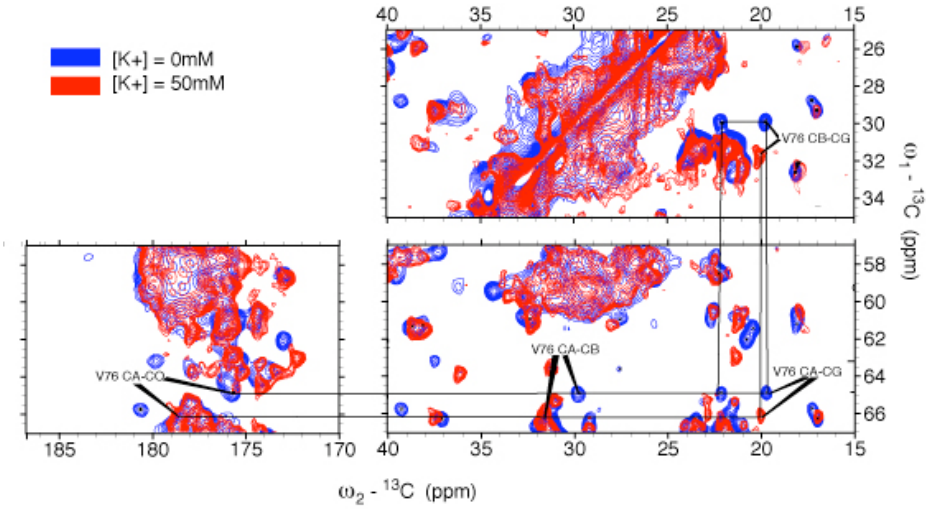


Fig. S6. V76 shows some of the most significant differences in chemical shift. V76 is at the heart of the selectivity filter. The figure shows $^{13}C$-$^{13}C$ 2D spectra of KcsA at 0 mM [K+] (blue) and 50 mM [K+] (red). All the carbon atoms on V76 show a change in chemical shift including CA, CB, CG1, CG2 and CO.

*Markers CA*

| [K+] in buffer | T74 | T75 | V76 | G77 | Y78 | G79 |
|---|---|---|---|---|---|---|
| 1uM | 61.28 | 62 | 64.88 | 48.41 | 60.97 | 47.45 |
| 10uM | 60.81 | 62.79 | 65.98 | 48.66 | 61.65 | 45.68 |
| 1mM | 60.93 | 62.8 | 65.8 | | 61.52 | 45.51 |
| 10mM | 60.73 | 62.6 | 65.92 | 48.35 | 61.47 | 45.09 |
| 50mM | 60.91 | 62.81 | 66.16 | 48.62 | 61.5 | 45.31 |
| 150mM | 61.02 | 62.94 | 66.34 | 48.61 | 61.48 | 45.42 |

*Markers CB*

| [K+] in buffer | T74 | T75 | V76 | G77 | Y78 | G79 |
|---|---|---|---|---|---|---|
| 1uM | 70.25 | 69.13 | 29.91 | - | 37.62 | - |
| 10uM | 69.62 | 69.12 | 31.72 | | 38.33 | |
| 1mM | 69.63 | 69.42 | 31.58 | - | 38.39 | - |
| 10mM | 69.72 | 69.22 | 31.65 | - | 38 | - |
| 50mM | 69.73 | 69.15 | 31.69 | - | 38.32 | - |
| 150mM | 69.9 | 69.19 | 31.73 | - | 38.3 | - |

*Markers CO*

| [K+] in buffer | T74 | T75 | V76 | G77 | Y78 | G79 |
|---|---|---|---|---|---|---|
| 1uM | 176.3 | 173 | 175.8 | | | 174.13 |
| 10uM | | | | | | |
| 1mM | | 172.7 | | | | 174.1 |
| 10mM | 176.3 | 172.5 | | | | 173.7 |
| 50mM | 176.2 | 172.3 | 178.74 | 174.1 | | 174 |
| 150mM | 176.3 | 172.5 | 178.9 | 174.5 | 178.3 | 174.4 |

*Markers N*

| [K+] in buffer | T74 | T75 | V76 | G77 | Y78 | G79 |
|---|---|---|---|---|---|---|
| 1uM | 98.78 | 108.95 | 120.1 | 101.1 | 115.22 | 100.6 |
| 1mM | | | | | | |
| 10mM | | | | | | |
| 50mM | 97 | 108.89 | 119.75 | 99.1 | 114.03 | 100.2 |
| 150mM | | | | | | |

Table S1. Carbon and Nitrogen chemical shifts of the selectivity filter residues of KcsA assigned at different [$K^+$]. Carbon is referenced to DSS externally via adamantane and Nitrogen is referenced externally to DSS via Glycine as described in the Methods. Chemical shifts are reported to 0.01 ppm, but interpreted with an error of 0.2ppm.

**Chemical Shift Prediction using SPARTA and SHIFTX:**

SPARTA and SHIFTX are is a chemical shift prediction programs that rely on a database of high resolution crystal structures and solution-state chemical shifts to predict the chemical shifts of a protein based on its crystal structure.

In order to validate the use of these tools for solid-state applications, we started by downloading published solid-state chemical shifts from the BMRB for the 4 structures shown in Table S1. The corresponding pdb file was downloaded from the RCSB-PDB database and input into SPARTA. The predicted chemical shifts were then compared to the experimental chemical shifts via two measures:

1) RMS as a measure of deviation

$$RMS = \sqrt{\frac{\sum (X_{pred} - X_{\exp})^2}{N}}$$

2) Pearson's R, as a scalar measure of linear dependence

$$R = \frac{\sum (X_{pred} - \overline{X_{pred}})(X_{\exp} - \overline{X_{\exp}})}{\sqrt{\sum (X_{pred} - \overline{X_{pred}})^2 (X_{\exp} - \overline{X_{\exp}})^2}}$$

| Bmrb code | Pdb ID | Resolution | Name | SCOP class/Fold | # of residues |
|---|---|---|---|---|---|
| 5757 | 1MU4 | 1.8 A | Crh dimer | Alpha and beta proteins/HPr-like | 84 |
| 15546 | 2ZUQ | 3.3 A | DsbB-ubiquinone | Alpha helical | 176 |
| 15380 | 2QMT | 1.05 A | GB1 | Alpha-beta/ubiquitin like | 56 |
| | 2NUZ | 1.85 A | SH3 | All beta/SH3 like barrel | 62 |

Table S2. List of protein structures/Assignments used for validation of SPARTA predictions when compared to solids-state assignments. The set was chosen based on availability of solid-state chemical shift lists and x-ray crystal structures collected under similar conditions of sample preparation.

| | NORMALIZED RMSD | PEARSON'S R |
|---|---|---|
| **Crh** | | |
| CA | 0.987 | 0.980 |
| CB | 1.123 | 0.996 |
| CO | 1.670 | 0.713 |
| N | 6.170 | 0.563 |
| | | |
| **GB1** | | |
| CO | 1.100 | 0.898 |
| CA | 0.931 | 0.982 |
| CB | 1.027 | 0.998 |
| N | 2.285 | 0.934 |
| | | |
| **SH3** | | |
| CO | 1.084 | 0.797 |
| CA | 1.071 | 0.960 |
| CB | 1.382 | 0.993 |
| N | 3.777 | 0.857 |
| | | |
| **DsbB** | | |
| CO | 1.358 | 0.575 |
| CA | 1.829 | 0.966 |
| CB | 0.907 | 0.997 |
| N | 2.314 | 0.863 |

Table S3. Normalized RMSD and Pearson's R for the available solid-state assignments when compared to predicted chemical shifts from SPARTA.

[$K^+$] dependent conformational changes in the selectivity filter of KcsA have been reported previously by X-ray diffraction and Electrophysiology. We compared the measured chemical shifts for all assigned marker peaks to the shifts predicted for various reported structures of KcsA. These x-ray structures used are listed in Table S3.

| PDB | Protein | Resolution | Buffer cond. |
|---|---|---|---|
| 1K4C | Mb-KcsA$^{+}$FAB | 2.0 A | 150mM KCl pH=5.4 |
| 1BL8 | Mb-KcsA | 3.2 A | 150mM KCl pH=5.4 |
| 3EFF | FL-KcsA$^{+}$2FAB | 3.8 A | 680mM $NH_4^+$ 300mM $Na^{+,}$ pH=5.7 |
| 1K4D | Mb-KcsA$^{+}$FAB | 2.3 A | 2mM KCl, 148mM NaCl pH=5.4 |
| 2ITC | Mb-KcsA$^{+}$FAB | 3.2 A | 50 mM MgAcetate, 150 mM NaCl, pH 7.0 |

Table S4. List of x-ray structures from the PDB that were used as input to predict chemical shifts that were compared to our experimental chemical shifts. All the structures are medium-low resolution. Our sample conditions are most consistent with 1K4C, 1BL8 and 1K4D.

The predicted chemical shifts from the 1K4C structure was compared to those of all of the other structures to see if RMSDs can be used pick out biologically significant changes. The overall RMSD of the entire protein is a poor indicator of significant changes in chemical shift, but the different structures show significantly different RMSDs for residues in the selectivity filter. Note that SPARTA is, in general, better at predicting CA and CB chemical shifts and less accurate at predicting N and CO chemical shifts.

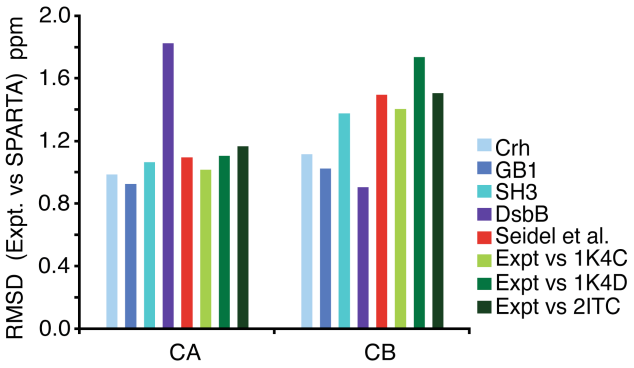


Fig. S7. The RMSDs that we report between our shifts and the SPARTA predicted shifts are well within the range of RMSDs reported for solid-state NMR chemical shifts. This figure shows the reported RMSDs at the Cα and Cβ sites of various different proteins whose solid-state chemical shifts are deposited in the BMRB (light blue: Crh, blue: GB1, teal: SH3, purple: DsbB), the average RMSD reported for all assigned proteins in the solid-state (red: Seidel et al.) and the RMSDs we report from our studies (light green: 1K4C vs 50mM $K^+$ shifts, green: 1K4D vs 0mM $K^+$ shifts, dark green: 2ITC vs 0mM $K^+$ shifts).

**Results from Elemental analysis of the pellet:**

| [K+] in buffer (added) | [K+] in buffer (measured) | [K+] pellet (AA) | [protein] pellet | ions per tetramer |
|---|---|---|---|---|
| 0 mM | 1 uM | 12 mM | 7.1 mM | 1.7:1 |
| 3 mM | - | 27 mM | 5.7 mM | 4.7:1 |
| 50 mM | 50.97 mM | 33 mM | 4.7 mM | 7.0:1 |

Table S5. Normalized RMSD and Pearson's R for the available KcsA structures when compared to 1K4C

The first column presents the concentration of [$K^+$] calculated stoichiometrically while preparing the buffer. The second column presents the actual [$K^+$] measured in the buffer solution via atomic absorption spectroscopy. The third column presents the [$K^+$] of potassium present in the ssNMR sample pellet as measured by atomic absorption spectroscopy. The volume used to calculate this concentration is the volume of the sample (30-60 ul). The fourth column presents the concentration of KcsA tetramer present in the pellet. This concentration was calculated based

on the initial amount of protein, measured by UV, that was added to the lipid before dialysis. Non-specific binding of $K^+$ has not been quantified.

**Hill Equation Fits:**

| $[K^+]$ | V76 (high K) | V76 (low K) | G79 (high K) | G79 (low K) | T74 (high K) | T74 (low K) |
|---|---|---|---|---|---|---|
| 0.001 | 0.69 | 0.31 | 0.41 | 0.59 | 0.42 | 0.58 |
| 0.01 | 0.25 | 0.75 | 0.33 | 0.67 | 0.6 | 0.4 |
| 1 | 0 | 1 | 0 | 1 | 1 | 0 |
| 10 | 0 | 1 | 0 | 1 | 1 | 0 |
| 50 | 0 | 1 | 0 | 1 | 1 | 0 |
| 150 | 0 | 1 | 0 | 1 | 1 | 0 |

Table S.6. The normalized populations at T74, V76 and G79 presented as a function of $[K^+]$.

We fit the population vs [K+] curves for V76, T74 and G79 using the standard hill equation

$$\Theta = \frac{[K^+]^n}{K_d + [K^+]^n}$$

$\Theta$ = fractional population
n = hill coefficient

We fit the data in two different ways,
1) let both Kd and n float
2) let Kd float and fix n to 1

For both cases, the model fit well for V76, but did not fit well for T74 and G79.

**V76**
The Hill equation, in this functional form, is a good fit for the V76 data because only one type of ligand.( K+) can bind at the V76 site, so there are no competitive kinetics. This is consistent with the idea that the internal site S2 is most selective for K+ and that Na+ cannot bind at this site.

Results from the fits:

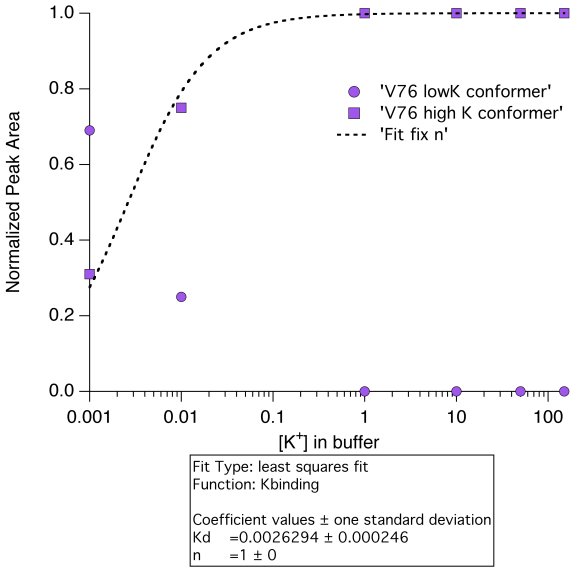


When n was fixed at 1
ChiSq = 0.003
$K_d$ = 2.6 ± 0.2 uM
n = 1

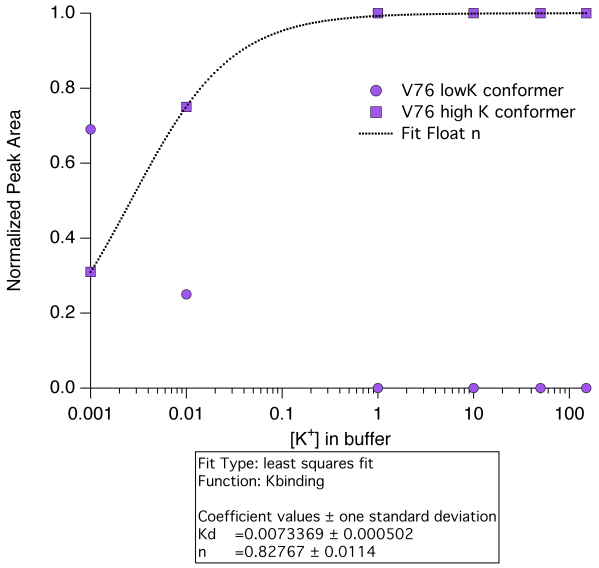


When both Kd and n were allowed to float
ChiSq = 5.5 x $10^{-5}$
$K_d$ = 7.3 ± 0.5 uM
n = 0.83

Fig. S8. This figure shows hill equation fits to the fractional populations at V76 as a function of whether or not we allow n to float.

**T74 and G79**

The Hill equation, in this functional form, is not a good description for binding kinetics at the peripheral sites, because at both these sites, (S1 and S4), both Na and K can bind at these sites and a simple picture fails to describe the kinetics.

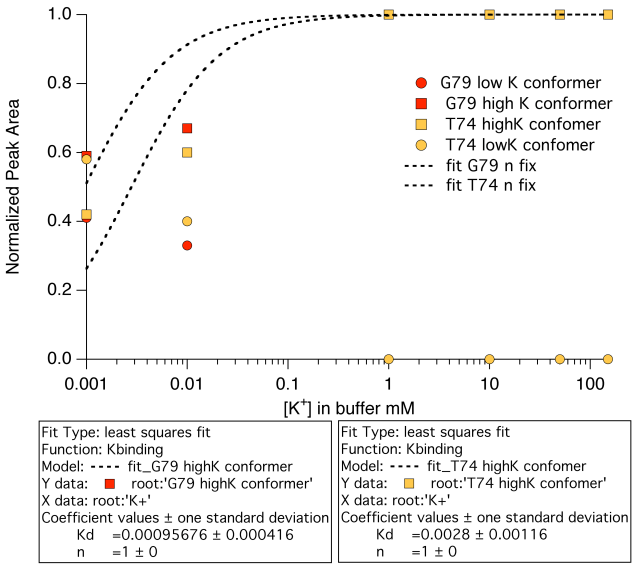


When n was fixed at 1

T74
ChiSq = 0.06
$K_d$ = 2.8 ± 1.1 uM
n = 1

G79
ChiSq = 0.07
$K_d$ = 1.0 ± 0.4 uM
n = 1

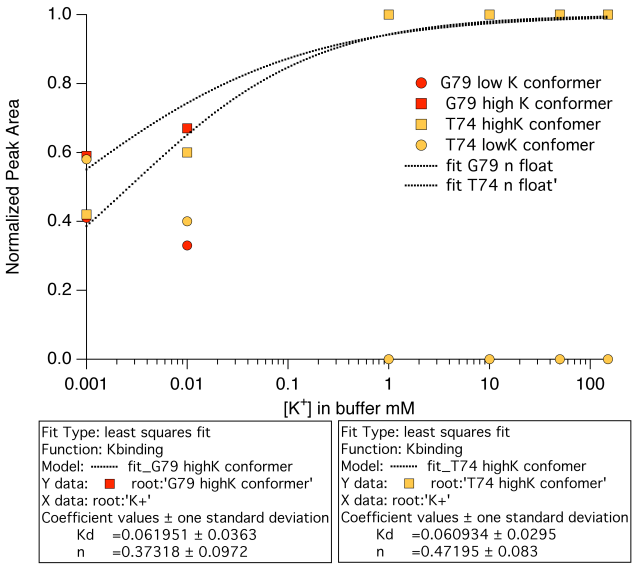


When both Kd and n were allowed to float

T74
ChiSq = 0.007
$K_d$ = 61 ± 29 uM
n = 0.47

G79
ChiSq = 0.01
$K_d$ = 62 ± 36 uM
n = 0.37

Fig. S9. This figure shows hill equation fits to the fractional populations at T74 and G79 as a function of whether or not we allow n to float.

In order to test the validity of our fits, we added a $[K^+]$ = 0 point to the data to see if this changed the results, since the lowest $[K^+]$ that we could reach experimentally was 1 uM. The plots had to be converted from logarithmic plots to linear plots, but the results were identical.

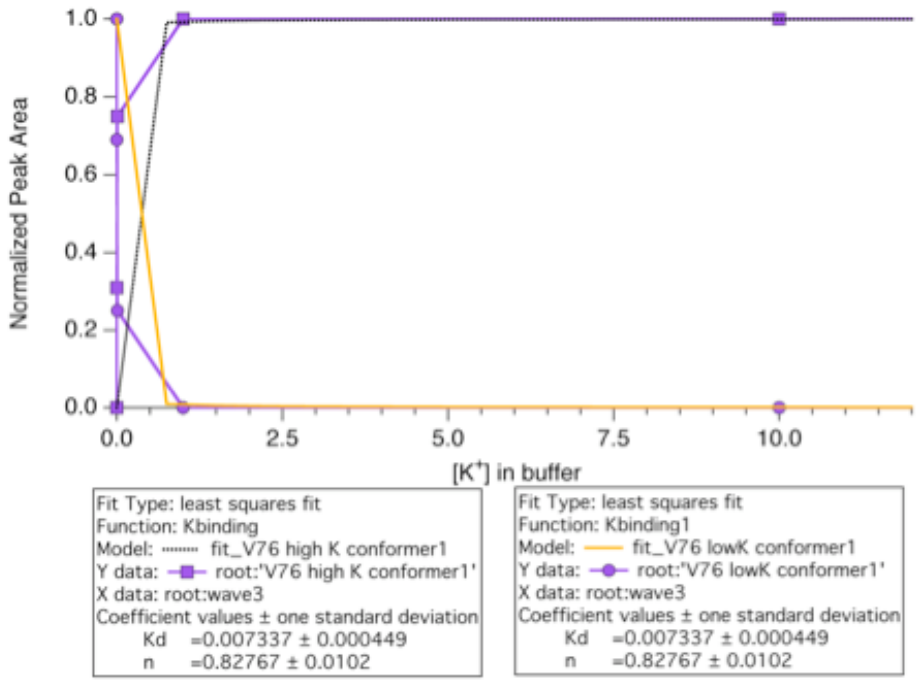


Fig. S10. This figure shows hill equation fits at V76 if we include a pure [K+] = 0 point. As shown by the fits, the values of Kd and n do not vary as

**Simulations with SPINEVOLUTION**

Input Parameters:
Static Field: 750 MHz
Chemical shift difference:
1.8ppm (shifts at -0.9 and 0.9) (for the V76 site)
0.4ppm (shifts at -0.2 and 0.2) (for the T74 site)
MAS: 14 KHz
Exchange rate: sampled from .05 to 2.5 Khz
Dwell: 100 us
Acquisition length: 1024 pts
Zerofill: 2048
T2 relaxation: 6ms

| csa_parameters | ani. | asym. | d11 | d22 | d33 |
|---|---|---|---|---|---|
| 1 | -23.9 | 0.29 | 10.2 | 5.6 | -15.9 |
| 2 | -23.9 | 0.29 | 10.2 | 5.6 | -15.9 |

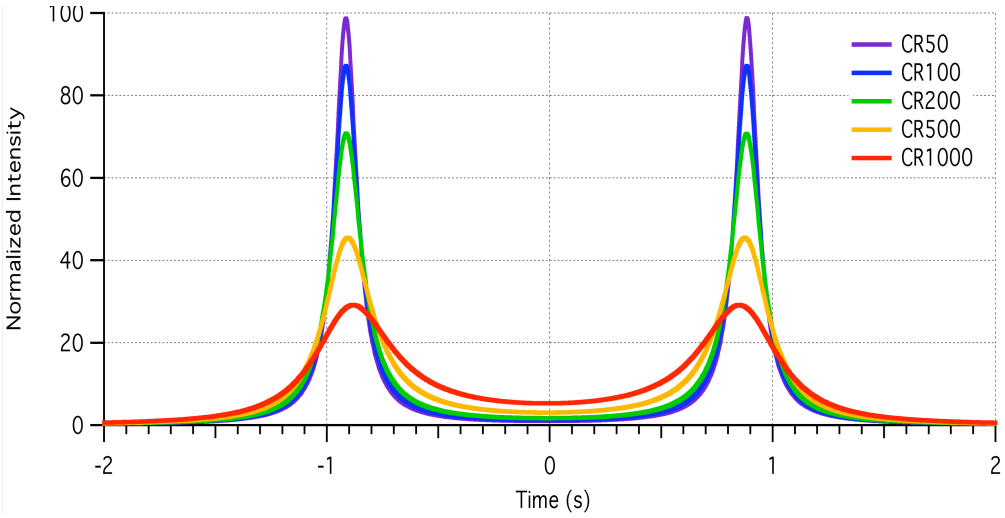


Figure S11. This figure shows a simulation of the V76 exchanging lineshape with CSA and R2 effects. Since we do not notice any appreciable line-broadening of these peaks in our spectra, we report that the rate is < 500/s based on this marker peak.

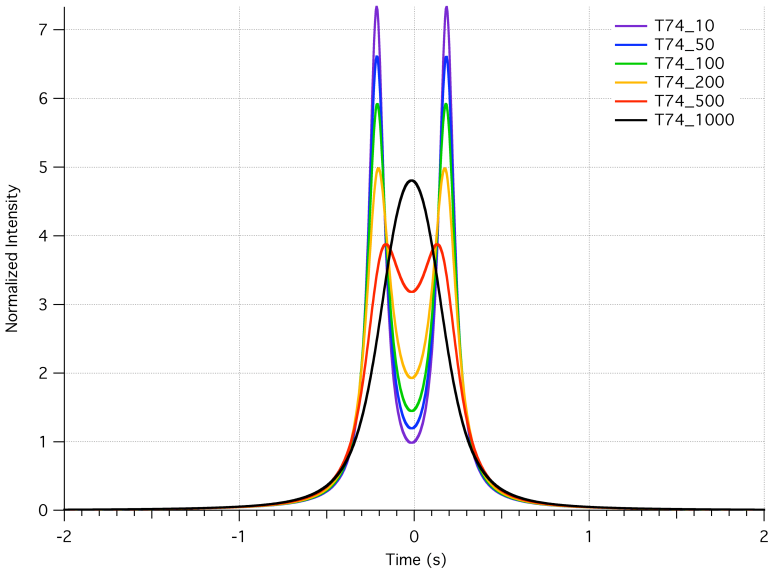


Figure S12. This figure shows a simulation of the T74 exchanging lineshape with CSA and R2 effects. Since we do not notice any appreciable line-broadening or coalescing of the peaks in our spectra, we report that the rate is < 500/s based on this marker peak.